

Light-sheet optimization for microscopy

Dean Wilding^a, Paolo Pozzi^a, Oleg Soloviev^{a,b}, Gleb Vdovin^{a,b}, and Michel Verhaegen^a

^aDelft Center for Systems and Control, Delft University of Technology, Mekelweg 2, 2628 CD Delft, the Netherlands

^bFlexible Optical B.V., Polakweg 10-11, 2288 GG Rijswijk, the Netherlands

ABSTRACT

Aberrations, scattering and absorption degrade the performance light-sheet fluorescence microscopes (LSFM). An adaptive optics system to correct for these artefacts and to optimize the light-sheet illumination is presented. This system allows a higher axial resolution to be recovered over the field-of-view of the detection objective. It is standard selective plane illumination microscope (SPIM) configuration modified with the addition of a spatial light modulator (SLM) and a third objective for the detection of transmitted light. Optimization protocols use this transmission light allowing the extension the depth-of-field and correction of aberrations whilst retaining a thin optical section.

Keywords: Adaptive optics, imaging, microscopy, light-sheet microscopy, optimization

1. INTRODUCTION

The light-sheet fluorescence microscope^{1,2} (LSFM) is gaining increasing reputation as a tool for biomedical research.³ The practical advantages of this microscope come from the combination of wide-field imaging speed with the optical sectioning ability of the confocal microscope.

The LS microscope is a trade off between the two methods and it works by delivering its illumination orthogonal to the fluorescence detection axis, therefore, only the imaged plane is illuminated, see Figure 1. This feature allows it to have lower photo-bleaching and toxicity when imaging samples than the confocal microscope.³ This makes the LSFM a highly efficient imaging technique with great future potential for biomedical research.

Since like in the confocal microscope the point-spread function (PSF) of the microscope is the product of the illumination profile and the detection PSF, to have the best axial resolution a thin light-sheet is required. A thin light-sheet is best generated using a high NA objective and cylindrical optics to limit the illumination of the back aperture in one direction. Due to the working distance of modern objective lens being much smaller than their size, a compromise to their NA must be made in order to place two of them orthogonally.

This spatial hindrance of placing two high numerical aperture (NA) objective lens orthogonally is a major drawback with LSFM. It imposes difficulties not only in limiting the resolution, but also in the preparation and mounting of samples and in the delivery of the illumination. LSFM in general are mounted and prepared in a different way to the vast majority of microscopy techniques.

Furthermore, when using a high NA objective lens to focus a laser beam the Gaussian beam waist, w_0 , is only quasi-uniform over a small range known as the Rayleigh range, z_R .⁴ Hence, for a high resolution in three dimensions it is required to use a small field-of-view (FOV), hereby limiting the applicability of this technique for many applications.

Whilst there have been attempts by changing the method of light delivery to circumvent this problem of spatial hindrance each with their own advantages and disadvantages,^{5,6} it invariably involves the loss of NA and subsequently image quality.

As a result of this LSFM tends to be used on larger specimens where the desire to image with the highest possible resolutions is not required, but to image fast and with reasonable quality. In this case, however,

Further author information: (Send correspondence to D.W.)

D.W.: E-mail: d.wilding@tudelft.nl, Telephone: +31 15 278 1758

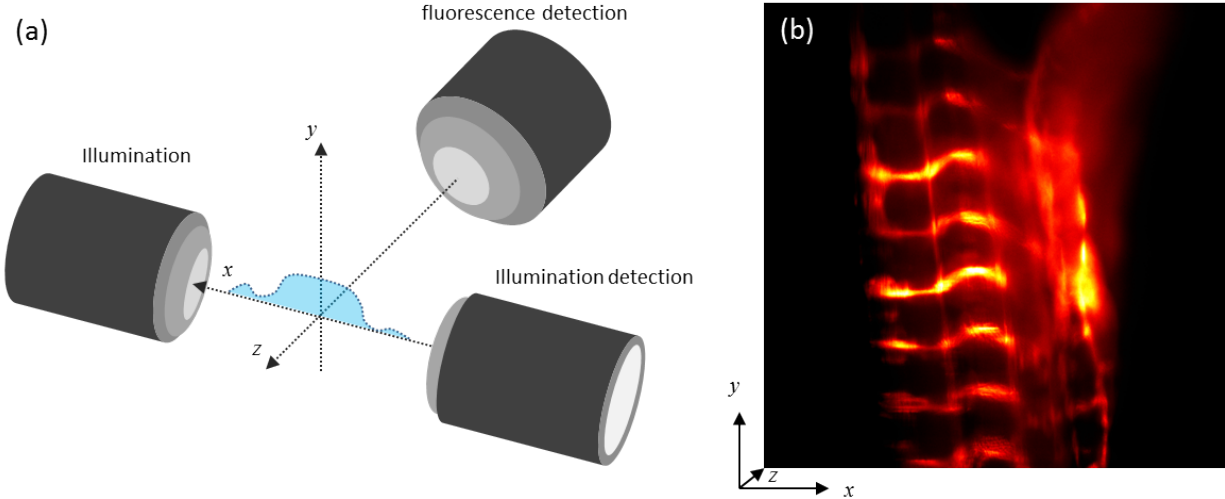


Figure 1. (a) A diagram showing the configuration of lens in the LSFM setup. The fluorescence is detected orthogonally to the illumination. (b) A standard LSFM image of a fixed Fli:EGFP zebrafish tail with matching coordinate axes.

the increase in the size of the samples increases the inhomogeneity of the optical path and thus degrades the performance of microscope. For this reason many of the larger samples are chemically treated⁷ or genetically modified⁸ before imaging to increase their transparency and optical quality.

In both these extremes it is clear that from both these regimes for the small scale and the larger scale, adaptive optics (AO), namely the ability to control the phase of the illumination light and the detection light would be beneficial to improve this technology. In this paper the use of adaptive optics in the illumination path and detection path of a LS microscope is presented alongside the use of wavefront shaping to improve the beam profile.

Adaptive optics in microscopy has the goal of improving the quality of the images that the microscope produces. One of the main approaches are called sensorless adaptive optics.⁹ In this case there is no direct sensing of the wavefront coming towards the camera, instead the image quality is organised into a mathematical form that can be optimized through a algorithm to ultimately yield an optimal solution: a “perfect image.”

LSFM uses wide-field (WF) imaging and therefore, the problem is made harder by the fact that we are imaging extended objects and not collecting from a single point as with confocal techniques. In the case of single point-like objects it is known what is desired, namely a diffraction-limited Airy disc. In wide-field imaging, the “perfect image” is not known making the problem all the more difficult to solve, since you do not know when you have found it.

Whilst it is possible to include fluorescent microspheres in the sample to act as artificial guide stars,¹⁰ it is not very practical for biological imaging in live tissues. The problems arise since alien material is introduced that causes a immune response from the organism, which is to be avoided if one wants to faithfully approximate the natural state in the microscope.

In such a sensorless framework, adaptive optics in the LSFM essentially wants to solve the following optimization problem, where σ is a metric that defines the quality of the images produced, for example, it could be the image sharpness or a measure of the high spatial frequency content of the image:

$$\max_{\phi, \varphi} \sigma \quad (1)$$

Here the pupil plane phase of the illumination objective, ϕ , and the fluorescence pupil plane phase, φ , as our control variables. The goal of the optimization is to find the phase patterns to apply in these pupils such that the image quality is maximized. In practice, however, this does not mean that we will have found the *perfect* image, but to the ability of the adaptive elements it will have been improved.

There are two broad approaches to the problem, one that is simply based on taking measurements on the experimental system until convergence and then the second makes a model of the system and uses that model to find the optimum without the need for measurement taking.

The model-free approach tries different possibilities on the system and sees which one is the best one to use. At this point it is worth making a note on the scale of this problem. For example, adaptive element with 250,000 actuators and 16-bit quantization running at 100Hz would take about four and a half years to search through every possibility and test them for suitability. Even if the system was stable over that time frame and noise-free, it would still be impractical therefore, another way must be found to compute the optimal value.

Hence people turn to optimization-based solutions, however, even for optimization-based approaches the peculiarities of optical systems make it the worst possible kind of problem to solve. Equation 1 is non-linear, non-convex, full of local minima and stationary points, and the measurements in general are noisy. This means that the problem such posed would not yield any meaningful results in the vast majority of cases. Nevertheless, approaches to sensorless adaptive optics have yielded promising results.^{11,12}

Hereby, there are two approaches to take: one in the case of small aberrations and another in the case of larger aberrations. Since with small aberrations it is reasonable to assume that the present state of the system without correction is close to the global maximum. In this case all the algorithm needs to do its make slight adjustments to the phase until the metric is maximized. This is a local optimization problem.

In the case of large aberrations, it is not possible to say that if the algorithm that converges to the nearest local maximum will indeed be the best possible option available. In this case it is necessary to use a global search algorithm. This approach is much slower and still there is no guarantee that it will converge to the global maximum.

Another way around the problem is to build a model of the system in question. It may be a completely theoretical model designed to mimic the operation of the system, or it may be a data-driven model that takes a certain number of measurements from the system and uses these to compute the optimum value.

Most often a model-based uses of measurements from the real world system. With this information a model is built and the optimization algorithm is run on the model. The advantages of the model-based approach is that it can often require less iterations and measurements than the model-free approach, by making the problem numerically easier to solve - such as a convex relaxation.¹³

Furthermore, model-based approaches by fitting can tackle the problem of noise better than model-free approaches making them more robust, and therefore, better in most situations. The downside of the model-based approach is that it requires time to develop the model and ensure that it operates in the same way as the system. It should only be considered if the performance of the model-free approach does not yield suitable results.

AO has been included into the LSFM^{14,15} with the focus on the correction of aberrations in the imaging arm. These approaches are a mixture of model-free and model-based approaches to correcting the aberrations. In this paper we will focus on the optimization of the illumination for use in the LSFM.

2. APPROACH TO AO IN LSFM

To better formulate the AO for LSFM it must be considered what sources of information that are available to measure the image quality metric. In the standard configuration of a LS microscope the only signal that is acquired are images of the fluorescence signal. From this data it is possible to compute an image quality metric σ , however, very little information is given about the thickness or the length of the LS in this approach.

In order to make the problem easier to solve we consider another imaging camera into the configuration. This camera measures the light that is transmitted through the sample. We are able to obtain an image of the beam via a confocal measurement. The image quality metric in some way contains this information, but if we are able measure it directly and therefore, it makes it easier to correct.

For the illumination light it is desired to have many degrees of freedom in the hope of correctly as many higher order aberrations as possible. Additionally, since the incident light is coherent it allows us to make use

of spatial light modulators (SLM). A nice additional advantage with these devices is that they have very high stroke lengths, since the phase can be wrapped, therefore, it is possible to use the SLM to also introduce the cylindrical focus.

On the detection side it is necessary to be able to control the focal plane of the microscope, in order to both change the focal plane and remove aberrations a deformable mirror is included in the fluorescence path. Hence, two adaptive components to control the phase in the two key pupils of the optical system. We have realized such as a system has been realised using a liquid-crystal phase only SLM (512x512, Boulder/Meadowlark, US) in the illumination path and a 69-actuator deformable mirror (DM) (DM69, Alpao, France). These two components allow full adaptive and wavefront control over the light in the LS microscope to the specifications of their design.

In Figure 2 the schematic of the experimental setup is shown. At the centre there is a custom designed and 3D printed acrylic (Shapeways, Netherlands) sample chamber with three ports for objective lenses (2x UMPLFLN 10x, 1x UMPLFLN 20x Olympus, Japan) sealed so that the chamber is water tight. The samples are mounted in agarose gels and suspended by glass capillaries above the samples. A 4D translation stage is used (USB Stage, Picard Industries, U.S.) for coarse sample movement and alignment. Fine adjustments of the illumination focus and LS position are done optically using tip-tilt and defocus actuation on the SLM with corresponding focal compensation on the DM. This ensures that the plane of the LS is coplanar with the detection objective focal plane.

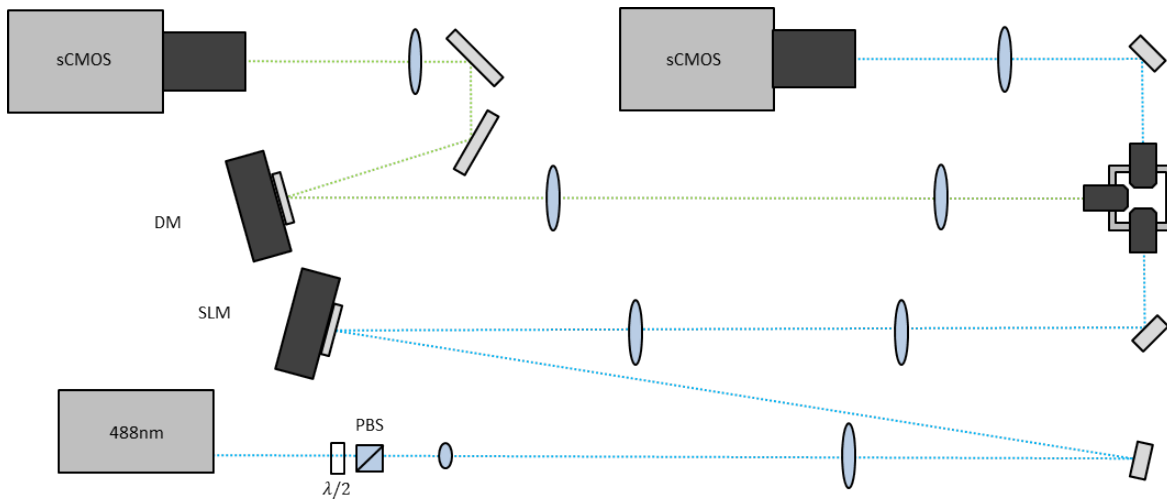


Figure 2. A schematic showing the realization of the system setup for full adaptive control of the LS microscope. A 488nm laser source is used to illuminate the SLM after polarisation control and expansion. The image of the SLM is conjugated with the back aperture of the illumination objective after zero order correction. The fluorescence light is collected and imaged on a sCMOS camera via the DM for focus and correction. The transmitted light is collected and used to feedback and control the illumination.

The fluorescence light is captured through the 20x objective is relayed onto the DM and captured on an sCMOS camera (Orca Flash 4, Hamamatsu Photonics, Japan). The transmission light is detected through an objective in confocal alignment with the illumination objective and imaged onto a CMOS camera (DCC1545M, Thorlabs, US). In addition, using the transmitted light on the camera the beam shape and quality can be adapted. Both the light captured by both the cameras is used for the optimization of the image quality.

The SLM is not conjugated to the back aperture of the illumination objective as would be conventional. In order to remove the effect of the zeroth order reflection from the SLM surface, a corrective procedure must be implemented. The corrector consists of a permanent defocus applied to the SLM and a beam blocking pinhead. Since the zeroth order light does not undergo the SLM phase change, it is focused by the first lens (AC508-180-A-ML, Thorlabs, U.S.) at the back focal plane and a pinhead is placed to block the light. The unblocked light containing the first order comes into focus around 50mm from the pinhead and is sufficiently defocused such that the performance of the SLM is not noticeable affected by this procedure. At this point a slit is placed to block

the second order light and to prevent the formation of the three LSs in the sample chamber. The second lens (AC508-180-A-ML, Thorlabs, U.S.) relays the image of the SLM, minus the defocus, onto the back aperture of the illumination objective. The illumination objective focal plane is therefore, conjugated with the first order of the SLM. Hereby, giving full control over the illumination light.

3. LIGHT-SHEET CORRECTION AND SHAPING

Before we shape the LS, the beam aberrations are minimized by the maximization of the variance of an region-of-interest (ROI) over the LS on the transmission camera. For the diffraction-limited Gaussian beam this method is adequate, however, for a more complex beam structure this will not converge to the optimum solution. The optimization is performed using a custom algorithm¹⁶ that is robust to the measurement noise and uses M Zernike modes as a basis for the SLM phase. With N pixels in the ROI, the optimization is mathematically described as:

$$\max_{\alpha} \frac{1}{N} \sum_{n=0}^N \left(I_n(\alpha) - \frac{1}{N} \sum_{n=0}^N I_n(\alpha) \right)^2 \quad (2)$$

Figure 3 shows the improvement in the beam profile at the focal position of the LS before and after correction using this technique. In this case the sample is 2% agarose gel in a glass capillary tube. Only $M = 5$ Zernike modes were used in correction on an ROI 64x64px and 100 iterations of the algorithm were run to ensure convergence.

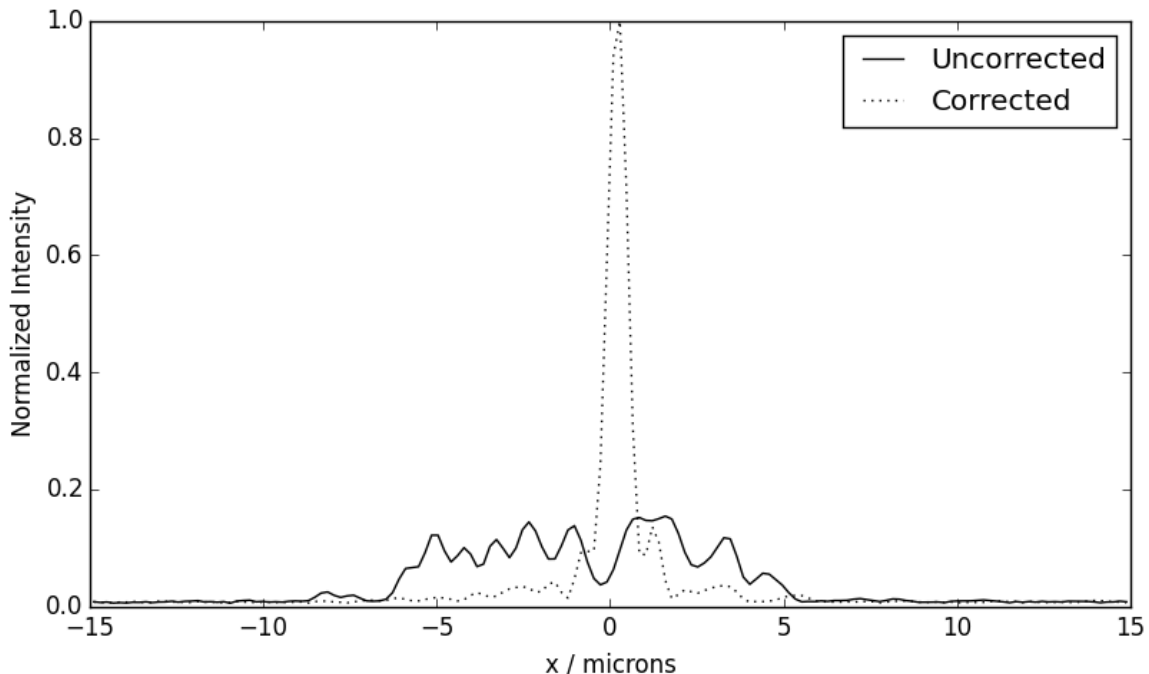


Figure 3. A plot of the beam profiles of the LS at the focus before and after correction. The sample, through which the LS passes, is agarose inside a glass capillary tube.

After this correction the LS is then shaped. As stated previously the profile of the standard Gaussian beam does not produce the optimum LS for imaging. The ideal LS for imaging would be as thin as possible and would be uniform in intensity and thickness over a long range. These are not the properties of the Gaussian beam which diverges from the focus decreasing the on axis intensity and increasing the out-of-focus light.

There have been already many approaches to this problem in the literature such as Bessel beams,¹⁷ Airy beams¹⁸ and aspheric systems.¹⁹ Here we take a different approach and form a metric for the quality of the LS.

Since the SLM allows us to shape the profile of the focal intensity by modifying the phase in the illumination pupil, we use wavefront shaping²⁰ to find our optimal LS. This mathematical problem is hugely under-determined due to phase diversity, that is there are many possible phase patterns that give the same intensity at the focal position. Therefore, to find the best phase profile on the SLM we have designed a metric that is suitable for the purpose of evaluating the quality of the LS. Images I_k are taken on the transmission camera at K positions over a range of Δ .

$$\text{r.m.s.} = \rho = \sqrt{\frac{1}{K} \sum_{k=0}^K (I_k - \max(I_k))^2} \quad (3)$$

The r.m.s. is essentially the deviation from the ideal LS. A LS that is flat along the optical axis has a value of zero. The range of Δ effects the number of positions are needed for the optimization to converge to the global minimum. A larger value of Δ requires more positions than a smaller value, this is due to the size of the PSF. The longer the range the blinder the metric becomes to non-ideal optimizers of the problem for the same number of measurements, i.e. there are more local minima for the algorithm to converge to.

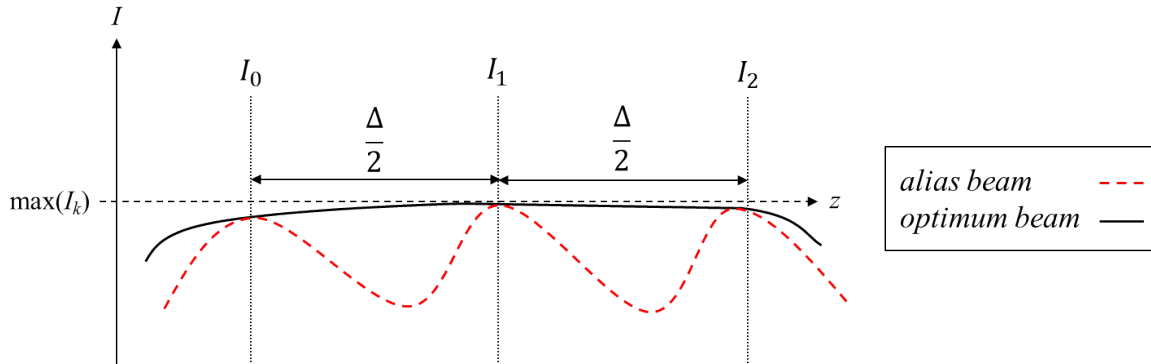


Figure 4. A visualization of the metric used to shape the beam profile. If an insufficient number of measurements is taken aliasing can occur in finding the solution.

Visually, with $K = 3$ it is possible to have a long flat axial section, or it is possible to have three humps. All of these will technically give the same value for the objective, but they will not be the solutions that we want to find.

Moreover, it is necessary to be very particular with the functions that one chooses to apply to the SLM in order to extend the depth of field. Whilst a common approach is to use cubic functions, this is not ideal for LSFM since the PSF becomes distorted and asymmetric. Furthermore, complex pupil functions in the general case tend to produce asymmetric axial PSFs.

Our approach uses binary pupil filters (PF)²¹ to provide an extended depth of field to the focused LS. Unlike other most other commonly used beam forming techniques, that is the Gauss-Bessel beam or the Gaussian beam it has a uniform axial profile along the sheet for a given range. The pupil function is real valued ± 1 and therefore, the solution is symmetric along the optical axis and in the orthogonal directions. These pupil filters are found by a two-stage optimization procedure²² of the step changes and are effective at keeping the axial resolution over the central range uniform. Essentially, the positions of the step changes m_i 's for M positions are optimized, where $\mathbf{m} \in \mathbb{R}^M$,

$$\begin{aligned} \min_{\mathbf{m}} \quad & \rho(\mathbf{m}, \Delta) \\ \text{s.t.} \quad & m_i + \delta < m_{i+1} \end{aligned} \quad (4)$$

Here δ is included as a constraint. This is the width of a Fresnel zone in the pupil, essentially, elements are closer than a Fresnel zone they will exhibit no influence on the shape of the focused beam. For this reason, it

is only possible to find solutions to the PF up to and including the number of Fresnel zones in the pupil. The profile along the direction of the light-sheet propagation is shown in Figure 5. Here the intensity is normalized so that they both have the same intensity at the focal position.

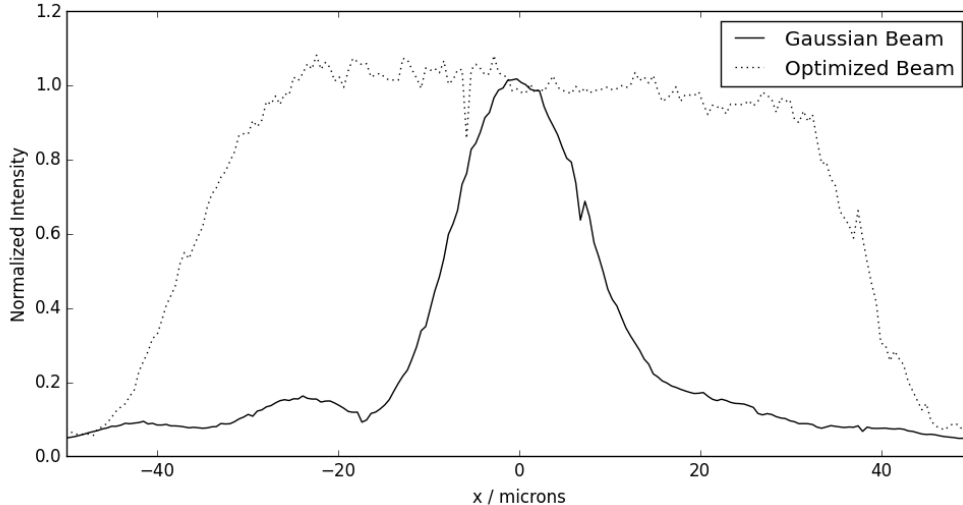


Figure 5. The x -axis profile of a LS as viewed from the fluorescence objective in the focal plane. The optimization of the pupil phase is able to extend the region over which the light-sheet is uniform.

The effect of the PF phase profile is to extend the region over which the beam is constant. In the example shown in Figure 5 a $4.2\times$ full-width at half-maximum (FWHM) axial extension for a $1.6\times$ increase in lateral beam size is seen. For comparison decreasing the NA by $1.6\times$ would only yield an increase of $2.6\times$ and it would not produce this flat intensity across the focal range. Equally, the PFs have the advantage that they are designed for the specific pupil and they are a phase only technique meaning no laser power is lost.

4. DISCUSSION

In this paper we have outlined how the use of adaptive optics to primarily control the illumination in a LS microscope may be implemented. We have discussed our experimental setup and our approaches to the shaping of optimal LS for LSFM and correction of aberrations introduced by the sample or the optical system.

The challenges that remain is to integrate the shaping and the aberration correction within thick and complex samples. With no correction the aberrations introduced by thick samples, such as zebrafish, mean that whatever wavefront shaping is applied to the LS it will be scrambled by the sample and appear in fluorescence no different to that of a Gaussian beam. Hence, increasing the number of spatial frequencies that can be corrected will bring better optical sectioning to the LSFM with thick samples.

Furthermore, it is not simply enough in the LS microscope to correct for the illumination alone. The light that is emitted from the sample has to pass through a large amount of refracting tissue before it reaches the detection camera. We have outline the approach that we have taken in this paper as the first steps towards the model-free WF correction in the LS microscope. We believe that the challenge lies in finding the correct metric for this approach, one that correlates well with the information content of the images. Once all of these elements are combined it should be possible for truly wide-field imaging to be performed in thick samples with confocal optical sectioning.

ACKNOWLEDGMENTS

This work is sponsored by the European Research Council, Advanced Grant Agreement No. 339681. The authors would like to thank the contributions of W.J.M. van Geest and C.J. Slinkman.

REFERENCES

- [1] Voie, A., Burns, D., and Spelman, F., “Orthogonal-plane fluorescence optical sectioning: Three-dimensional imaging of macroscopic biological specimens,” *Journal of microscopy* **170**(3), 229–236 (1993).
- [2] Huisken, J., Swoger, J., Del Bene, F., Wittbrodt, J., and Stelzer, E. H., “Optical sectioning deep inside live embryos by selective plane illumination microscopy,” *Science* **305**(5686), 1007–1009 (2004).
- [3] Santi, P. A., “Light sheet fluorescence microscopy a review,” *Journal of Histochemistry & Cytochemistry* **59**(2), 129–138 (2011).
- [4] Born, M. and Wolf, E., [*Principles of Optics*], Cambridge University Press.
- [5] Tokunaga, M., Imamoto, N., and Sakata-Sogawa, K., “Highly inclined thin illumination enables clear single-molecule imaging in cells,” *Nature methods* **5**(2), 159–161 (2008).
- [6] Dunsby, C., “Optically sectioned imaging by oblique plane microscopy,” *Optics express* **16**(25), 20306–20316 (2008).
- [7] Dodt, H.-U., Leischner, U., Schierloh, A., Jährling, N., Mauch, C. P., Deininger, K., Deussing, J. M., Eder, M., Zieglgänsberger, W., and Becker, K., “Ultramicroscopy: three-dimensional visualization of neuronal networks in the whole mouse brain,” *Nature methods* **4**(4), 331–336 (2007).
- [8] White, R. M., Sessa, A., Burke, C., Bowman, T., LeBlanc, J., Ceol, C., Bourque, C., Dovey, M., Goessling, W., Burns, C. E., et al., “Transparent adult zebrafish as a tool for in vivo transplantation analysis,” *Cell stem cell* **2**(2), 183–189 (2008).
- [9] Booth, M. J., “Adaptive optics in microscopy,” *Philosophical Transactions of the Royal Society A: Mathematical, Physical and Engineering Sciences* **365**(1861), 2829–2843 (2007).
- [10] Azucena, O., Crest, J., Kotadia, S., Sullivan, W., Tao, X., Reinig, M., Gavel, D., Olivier, S., and Kubby, J., “Adaptive optics wide-field microscopy using direct wavefront sensing,” *Optics letters* **36**(6), 825–827 (2011).
- [11] Débarre, D., Botcherby, E. J., Watanabe, T., Srinivas, S., Booth, M. J., and Wilson, T., “Image-based adaptive optics for two-photon microscopy,” *Optics letters* **34**(16), 2495–2497 (2009).
- [12] Booth, M. J., “Wavefront sensorless adaptive optics for large aberrations,” *Optics letters* **32**(1), 5–7 (2007).
- [13] Antonello, J., van Werkhoven, T., Verhaegen, M., Truong, H. H., Keller, C. U., and Gerritsen, H. C., “Optimization-based wavefront sensorless adaptive optics for multiphoton microscopy,” *JOSA A* **31**(6), 1337–1347 (2014).
- [14] Bourgenot, C., Saunter, C. D., Taylor, J. M., Girkin, J. M., and Love, G. D., “3d adaptive optics in a light sheet microscope,” *Optics express* **20**(12), 13252–13261 (2012).
- [15] Masson, A., Escande, P., Frongia, C., Clouvel, G., Ducommun, B., and Lorenzo, C., “High-resolution in-depth imaging of optically cleared thick samples using an adaptive spim,” *Scientific reports* **5** (2015).
- [16] Verstraete, H. R. G. W., Wahls, S., Kalkman, J., and Verhaegen, M., “Model-based sensor-less wavefront aberration correction in optical coherence tomography,” *Optics Letters* (2015).
- [17] Planchon, T. A., Gao, L., Milkie, D. E., Davidson, M. W., Galbraith, J. A., Galbraith, C. G., and Betzig, E., “Rapid three-dimensional isotropic imaging of living cells using bessel beam plane illumination,” *Nature methods* **8**(5), 417–423 (2011).
- [18] Vettenburg, T., Dalgarno, H. I., Nylk, J., Coll-Lladó, C., Ferrier, D. E., Čižmár, T., Gunn-Moore, F. J., and Dholakia, K., “Light-sheet microscopy using an airy beam,” *Nature methods* **11**(5), 541–544 (2014).
- [19] Saghafi, S., Becker, K., Hahn, C., and Dodt, H.-U., “3d-ultramicroscopy utilizing aspheric optics,” *Journal of biophotonics* **7**(1-2), 117–125 (2014).
- [20] de Visser, C. C. and Verhaegen, M., “Wavefront reconstruction in adaptive optics systems using nonlinear multivariate splines,” *JOSA A* **30**(1), 82–95 (2013).
- [21] Sheppard, C. J., “Pupil filters for generation of light sheets,” *Optics express* **21**(5), 6339–6345 (2013).
- [22] Wilding, D., Pozzi, P., Soloviev, O., G, V., Sheppard, C. J., and Verhaegen, M., “Pupil filters for extending the field-of-view in light-sheet microscopy,” *Optics Letters* (2016, in review).